B1 mapping of an 8-channel TX-array over a human-head-like volume in less than 2 minutes: the XEP sequence

A. Amadon[1], N. Boulant[1], M. A. Cloos[1], E. Giacomini[1], C. J. Wiggins[1], M. Luong[2], G. Ferrand[2], and H-P. Fautz[3]
[1]Neurospin, CEA/DSV/I2BM, Gif-sur-Yvette, France, [2]IRFU, CEA/DSM, Gif-sur-Yvette, France, [3]Siemens Healthcare, Erlangen, Germany

Introduction: Efficient mitigation of the RF inhomogeneity at high field using transmit coil arrays relies on the knowledge of the individual B_1 maps. As the number of transmit channels increases, so does the acquisition time of all maps. For in-vivo experiments, it is crucial to minimize this time of calibration, and several B1-measuring techniques compete to reach that goal. Here we focus on a fast 2D sequence proposed by Fautz et al.[1]. This reference deals with a single slice B1-map. It uses a non- or weakly-selective saturation pulse which produces a spatial–dependent flip-angle (FA) $\alpha(r)$ to be measured. Without magnetization preparation, a reference image is obtained from the selective excitation, which is used to divide the saturated image to obtain a map of $\cos \alpha$. While only one reference image is needed, the scheme is repeated for all coil elements under investigation, with a repetition time long enough for full T1 relaxation of all tissues in the sample. Here we extend the method to multi-slice imaging by using very selective pulses for both saturation and excitation, followed by an EPI echo train for readout. We then compare the performance of our so-called XEP sequence (short for "multiple transmission multi-slice B1-mapping technique with Echo Planar readout") with that of the 3D Actual Flip angle Imaging (AFI) sequence [2], known to yield accurate results when spoiling is properly addressed [3].

Method: We compared XEP and AFI performances on a Siemens 7T Magnetom scanner (Erlangen, Germany), equipped with an 8-channel transmit array feeding eight 1-kW RF power amplifiers. The AC84 gradient head coil allowed gradient amplitudes up to of 50mT/m and slew rate of 400T/m/s. A home-made transmit-array head coil was used, which consists of 8 stripline dipoles distributed every 45 degrees on a cylindrical surface of 27-cm diameter. Measurements were performed on a 16-cm spherical oil phantom with T1 measured around 600 ms. Special care was brought to B0-shimming in a combined mode. Then 3D B1-maps of the entire phantom were obtained for each channel using the AFI sequence [2] including its spoiling improvements [3]. The sequence parameters were: 1.28-ms square pulse, TR1/TR2= 33/167 ms, 6-mm isotropic resolution with a 32x32x28 matrix. Thus, the whole set of AFI acquisitions took 24 minutes for 8 channels.
For the XEP sequence, a highly selective minimum phase SLR pulse [4] with large time-to-bandwidth product (TBW = 15) was chosen to avoid slice interferences during the multi-slice imaging process. Its asymmetry with maximum energy at the end of the pulse also reduced the effective duration between the saturation and excitation pulses (TD << T1), providing better accuracy in the FA outcome [1]. Moreover, the SLR pulse was VERSE'd [5] around its peak in order to limit its duration to less than 10 ms, considering the limited power that could be used on a single Tx-channel. The excitation pulse was a 3-ms apodized sinc pulse with TBW = 20, whose slice profile had to fit tightly within the saturation pulse profile to avoid introducing wrong FA components from the borders of the saturation slice. Its thickness was chosen to be 4.5 mm while that of the saturation pulse was 6 mm. A single-shot EPI readout and an over-killing TR of 10 s between channel commutations were used, in order for the longitudinal magnetization to regrow to its full static value. 28 slices were interleaved during the TR period, so as to match the resolution and Field-Of-View of the AFI sequence. The overall sequence only lasted 1.5 min for all 8 channels, the first measurement being reserved for the reference image. In order to get good SNR through the whole volume, a combined excitation was played with appropriate phase on each channel to achieve a static RF shim mode [6] in the sample. These individual static phases were determined thanks to B1-phase maps acquired for each channel with a traditional FLASH sequence, in a preliminary step taking less than 30 seconds for all 8 channels.
For absolute FA-map comparison between AFI and XEP sequences, we used the same RF pulse integrals, which were chosen to cover a large dynamic range of FA, up to ~150° and higher. For this high-FA measurement to be possible (beyond $acos(-TR1/TR2)$ for AFI, and 90° for XEP), in both techniques, the sign of the ratio r of amplitude images to be divided had to be known. This was determined by considering and subtracting their associated phase maps. Also in both methods, the raw data were filtered in the same way to avoid Gibbs ringing.

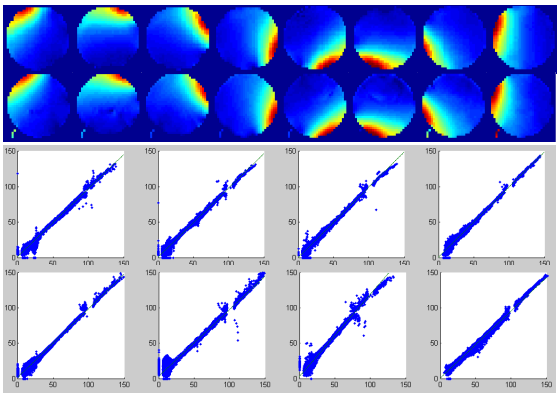

Fig. 1: Flip angle measurement of the phantom's central axial slice for each of the eight transmit coil elements. Top row: FA images from the AFI sequence; second row: same from the XEP sequence. Measured angles go up to 150°. Bottom rows: AFI versus XEP FA-values (in °) for all voxels in the phantom volume (AFI along horizontal axes). Fitted slopes range from 0.94 to 0.99, except for channel-7's.

Results and discussion:
In Fig. 1, FA-maps of the central axial slice of our phantom are shown, from the AFI and XEP sequences. The bottom rows show the associated scatter plots of the FA's found by both methods in every voxel of the phantom. A good agreement is achieved between the two techniques, with correlation coefficients reaching 0.99 for all scatter plots. But as expected, low FA values have a wider spread resulting from lower SNR and ill-determined *acos* when r approaches 1 in either method. Indeed the XEP method introduces a residual Nyquist ghost somewhat visible on some images, which probably brings poor precision at low FA's. This could probably be improved by using combined transmission methods such as [7] to recover a better accuracy in zones far away from the individual coil elements. However, for XEP, a separate, but short, acquisition would be necessary to get the phase maps out of the combined modes, as the phases after the SLR pulse are destroyed by the saturation spoiling process. This could be done in the preliminary step instead of FLASH'ing the individual coil elements, assuming the vector combination for the RF shim mode is known from previous similar exams.
AFI versus XEP FA-values show a linear trend as expected (straight line fits are overlaid on scatter plots), with slopes ranging from 0.94 to 0.99, except for channel 7 which has a slope of 1.16; another measurement with slightly lower pulse integral yielded a 1.0 slope for that channel; in fact, RF power amplifier non-linearity problems were later found at high voltage on it. This shows that both approaches lead to comparable scaling of the FA, within a ~5 % accuracy range. On the scatter plots, for the AFI sequence, a gap is visible in the data around 101°, corresponding to $r = 0$, which is never reached because of intrinsic noise always present in the TR2 image. The same effect is not as visible around 90° with the XEP data because of higher SNR in that case. It should also be stressed that XEP is significantly less SAR-demanding than AFI, allowing more than a 12-fold increase in speed of acquisition, while preserving a higher SNR.

Conclusion: Excellent convergence is reached between the XEP and AFI sequences for the FA relative spatial distributions. A better than 5 % uncertainty was found in the scaling of one technique with respect to the other. In terms of speed and SAR constraints, the XEP sequence greatly outperforms AFI for whole volume B1-mapping in the context of parallel transmission.

References: [1] H-P. Fautz et al., ISMRM 16 (2008), p.1247. [2] V.L. Yarnykh, MRM 57: 192-200 (2007). [3] K. Nehrke, MRM 61 : 84-92 (2009). [4] J. Pauly et al., IEEE Trans. Med. Imag. 10(1):53-65 (1991). [5] M.A. Bernstein et al., Handbook of MRI Pulse Sequences, Elsevier (2004), p. 58. [6] G. McKinnon et al., ISMRM 15 (2007), p. 173. [7] D.O. Brunner et al., ISMRM 16 (2008), p. 354.